Chemistry & Biology
Article

Engineering Unnatural Nucleotide Specificity to Probe G Protein Signaling

Fabien Vincent,[1,2] Silas P. Cook,[1] Emmanuel O. Johnson,[1] Dana Emmert,[1] and Kavita Shah[1,*]
[1]Department of Chemistry, Purdue University, 560 Oval Drive, West Lafayette, IN 47907, USA
[2]Present address: Renovis, Inc., 2 Corporate Drive, South San Francisco, CA 94080, USA.
*Correspondence: shah23@purdue.edu
DOI 10.1016/j.chembiol.2007.08.006

SUMMARY

G proteins comprise ~0.5% of proteins encoded by mammalian genomes. To date, there exists a lack of small-molecule modulators that could contribute to their functional study. In this report, we present the use of H-Ras to develop a system that answers this need. Small molecules that allow for the highly specific inhibition or activation of the engineered G protein were developed. The rational design preserved binding of the natural substrates to the G protein, and the mutations were functionally innocuous in a cellular context. This tool can be used for isolating specific G protein effectors, as we demonstrate with the identification of Nol1 as a putative effector of H-Ras. Finally, the generalization of this system was confirmed by applying it to Rap1B, suggesting that this method will be applicable to other G proteins.

INTRODUCTION

The human genome contains more than 160 G proteins [1], encompassing small G proteins, translation-elongation factors, and the α subunits of heterotrimeric G proteins. With the exception of elongation factors, they act as precisely engineered molecular switches and are deeply woven into the signal transduction network [2]. Small G proteins consist of an invariant core—the guanine nucleotide-binding domain coupled to the switch I and II areas regulating interactions with other macromolecules—and variable N and C termini additions specific to each enzyme [2]. Binding of GTP or GDP locks G proteins into dissimilar "on" and "off" conformations, respectively, and thereby regulates their affinities to other proteins (effectors) and initiates signaling cascades (Figure 1A). Their cycling between GDP- or GTP-bound conformations is controlled by GTPase-activating proteins (GAPs), GDP-dissociation inhibitors (GDIs), and guanine nucleotide-exchange factors (GEFs). These proteins determine the amount of GTP-bound enzyme available to bind to effectors and thus ultimately control the amplitude and duration of the downstream signals (Figure 1A).

A wide variety of diseases have their roots in deregulated G protein activities or have harmful signals conveyed through them [3–5]. Despite their great potential as drug targets, no active-site inhibitors are known to date. Traditionally, the high affinity of G proteins for their substrates (K_D of ~10 pM) and the high intracellular concentration of GTP (~1 mM) have been blamed for this failure [6]. The lack of such tools to allow for specific and temporal control over the activities of G proteins has prevented the contribution of small molecules to the elucidation of their pathways [7]. This is in sharp contrast with kinases, in which the availability of even partially selective inhibitors greatly facilitated their functional study in cellular systems [8].

The convergent engineering of small-molecule/protein interfaces to address biological questions has emerged as a powerful new tool [9]. This strategy allows for tight control over the biological activity of a desired protein by combining the advantages of both chemistry and genetics. Diverse systems have been studied by using this orthogonal chemical-genetic methodology including 7-transmembrane receptors [10], nuclear hormone receptors [11], methyl transferases [12], chemical inducers of dimerization [13], kinases [14, 15], and myosin [16].

G proteins themselves were the object of pioneering chemical-genetic studies [17]. A change in substrate specificity from GTP to XTP (xanthosine 5′-triphosphate) was achieved by mutating a conserved aspartate residue (D119 in H-Ras) interacting with the exocyclic C(2) amine of GTP to asparagine. The protein-nucleotide hydrogen bond thus abolished could be reestablished if XTP was used rather than GTP. This system was used to transform several G proteins into XTPases and enabled their study in in vitro systems [18]. However, XTP production occurs spontaneously in cells and is postulated to be mutagenic, as noncanonical nucleotides can be incorporated into nucleic acids [19]. Accordingly, a cellular protection mechanism that employs NTPases keeps XTP intracellular concentrations at a very low level, which is inadequate for the proper function of the modified G proteins [20]. Due to the low intracellular concentrations of XDP and XTP, the mutant enzyme therefore still binds GDP and GTP in vivo. Since the affinity of XTPases toward their natural substrates GDP and GTP is decreased by three orders of magnitude, the "on" and "off" switch mechanism is rendered ineffective and is replaced by a binding equilibrium [21]. As GTP is much more abundant than GDP, the majority of the mutant enzyme is in the GTP-bound form, thus making it constitutively active and rendering the application of this approach to in vivo studies impractical [21]. As a result, the design of a mutant G protein retaining its

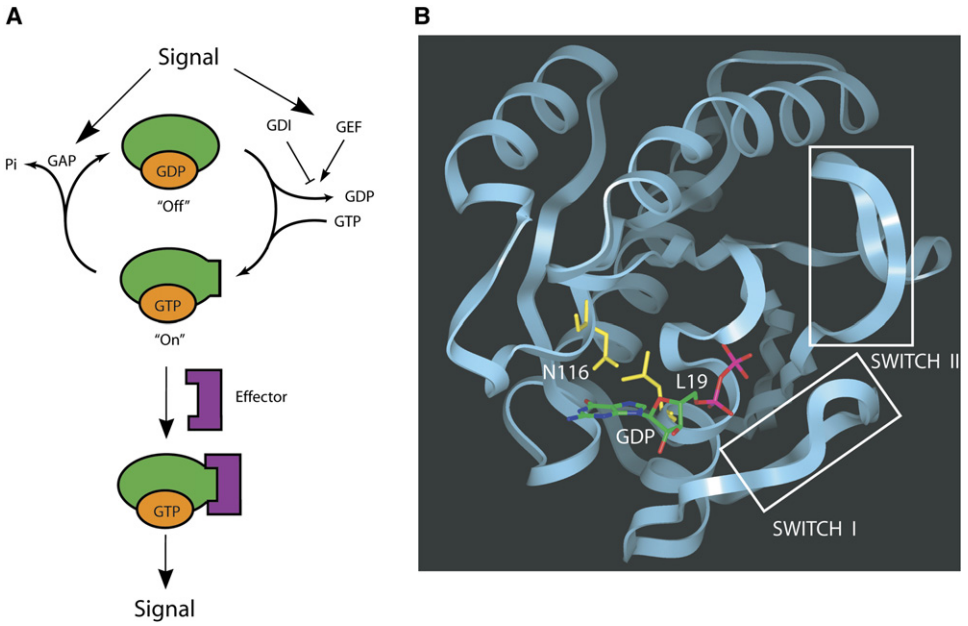

Figure 1. G Protein Function and Structure

(A) Schematic representation of small G protein signaling. Upstream signals are conveyed to G proteins through GDI, GAP, and GEF proteins. The conformational change due to GTP binding allows effectors to bind the G protein-GTP complex and conveys the signal downstream.

(B) Ribbon representation of H-Ras bound to GDP; amino acids L19 and N116 are highlighted along with the switch I and II regions.

natural nucleotide selectivity but susceptible to specific orthogonal small molecules is highly desirable [7].

We report, herein, the rational design and engineering of a system that allows for the specific inhibition or activation of, potentially, any G protein of interest. The key feature is the introduction of a subtle but unique structural distinction between the nucleotide-binding site of a chosen G protein and those of all other G proteins. This distinction was accomplished by introducing a space-creating mutation in the active site of the G protein. Using H-Ras as a model system, we show that the mutant protein remains fully functional, as it not only binds to its natural ligands GDP and GTP, but also retains the ability to undergo conformational changes in order to bind downstream effectors exactly like the wild-type (WT) enzyme. To complement this pocket, a panel of GDP and GTP analogs bearing various bulky groups at C(7) was synthesized. Two specifically designed orthogonal GDP and GTP analogs that uniquely bind to the engineered G protein and allow precise "on" and "off" control over its activity were identified. Modeling studies revealed the specific interactions responsible for the affinity and selectivity of these orthogonal molecules for the mutant protein. This precise control over G protein activity further led to the selective and efficient enrichment of H-Ras effectors from whole-cell lysate. Data obtained by using this approach lead us to propose Nol1, a protein whose overexpression in a variety of tumors correlates with poor prognosis, as a putative novel effector of H-Ras. Importantly, we show that the specific interactions engineered for H-Ras can be transferred to other G proteins in a straightforward manner, with the compounds designed in this study tightly controlling their activities. As the residues mutated are highly conserved across the G protein superfamily, three-dimensional structural information is not required, and this approach should thus be widely applicable.

RESULTS

Enzyme and Small-Molecule Design

Sequence alignments and structural studies have revealed the close similarity in the nucleotide-binding pockets of different G proteins [22]. This suggested the feasibility of designing an orthogonal small-molecule/enzyme system transposable to other members of this superfamily. Drawing from our experience with kinase engineering, we identified the much tighter ($\sim 10^5$-fold) affinity of guanine nucleotides for G proteins compared with that of ATP for kinases as the main technical hurdle.

We chose H-Ras as our model system since earlier studies have illustrated both GDP- and GTP-binding modes (Figure 1B) [2]. To design such a system, multiple criteria had to be satisfied. For the mutant protein these criteria were as follows: (1) an additional binding pocket had to be created in the active site, (2) the ability to bind GDP and GTP had to be conserved, (3) the ability to bind its upstream and downstream effectors had to be preserved, (4) it had to be functionally indistinguishable from its WT counterpart in cells, and (5) the mutations had to be in a conserved locus so that they could be translated to other G proteins. Orthogonal small molecules had

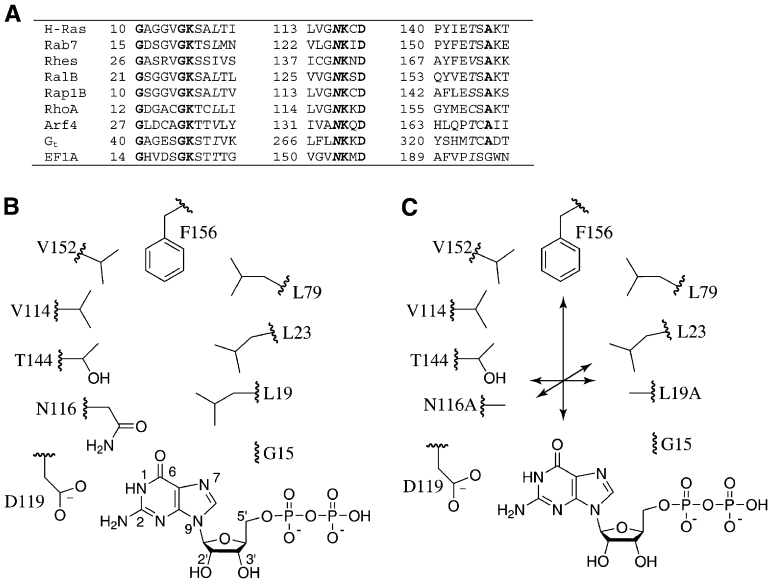

Figure 2. Protein Engineering Design

(A) Sequence alignment of the areas of diverse G proteins in close contact with the guanine ring system. Conserved residues are highlighted in bold, while L19, N116, and T144, residues discussed in this study, are italicized.

(B) Schematic representation of GDP binding to H-Ras WT. Amino acid side chains discussed in the text are numbered.

(C) Representation of H-Ras 19A-116A bound to GDP. The hydrophobic pocket created by combinations of L19 and N116 mutations to alanine or glycine has approximate dimensions of 10 Å in length and 3–6 Å at the entrance, depending on the combination of mutations.

several requirements to satisfy as well: (1) they had to possess greater affinity than GDP and GTP for the mutant protein to be able to compete with them in a cellular environment, (2) they could not bind to the WT G protein, even at high concentrations, and (3) their binding had to have a defined effect on the mutant enzyme by turning it selectively into the "on" or "off" conformation.

Accordingly, we conducted initial modeling studies for the rational design of mutant H-Ras proteins possessing an additional binding pocket in the active site and of small molecules complementing this additional pocket. The residues considered for mutagenesis had to be located near the guanine ring system but be far removed from the switch I and II areas that surround the GTP γ phosphate. These criteria suggested the mutation of L19, N116, or both. Importantly, these residues are highly conserved in other family members (Figure 2A) [23]. All of the members of small G protein (159 members) and heterotrimeric G protein superfamilies (16 members) lack alanine or glycine at these two positions (L19, N116) [24]. While the function of L19 has not been studied previously, N116 is believed to help stabilize the nucleotide-binding pocket [25]. Since they are on the backside of this binding site, they are away from the regions involved in conformational changes and effector binding, and their replacement was likely to have minimal impact on H-Ras function. Furthermore, we noticed the presence beyond them of a pocket lined with hydrophobic residues (Figure 2B). We postulated that the combined mutation of these two residues to either glycine or alanine would produce mutants possessing hydrophobic cavities of various sizes and shapes (Figure 2C). Importantly, D119, a key residue selecting for GTP over ATP and other nucleotides by hydrogen bonding to both the N(1) nitrogen and the C(2) exocyclic amine, was left untouched by this design.

To complement these mutations, we envisioned that molecules bearing bulky lipophilic moieties attached to GDP or GTP scaffolds might be able to target the newly created hydrophobic pocket. Using GDP and GTP as our compound scaffolds ensured that the orthogonal small molecules would probably use similar binding modes and therefore inactivate or activate the mutant enzyme, respectively. Furthermore, having the natural substrates as our chemical templates increased the likelihood of producing compounds with a similar affinity as a starting point. The incorporation of bulky substituents was expected to help fulfill two important criteria. First, these large groups would ensure very selective binding to the mutant enzyme since severe steric clashes would occur with the WT enzyme. Second, the additional hydrophobic interactions secured by the insertion of these groups in the hydrophobic pocket were predicted to selectively increase the affinity of the analogs, but not that of GDP/GTP, for the mutant protein. Accordingly, substitutions were made at either the C(6) or N(7) position of the guanine ring system; these substituents face the newly introduced cavity (Figure 2C). For the second class of compounds, the N(7) nitrogen atom had to be exchanged for a carbon atom since its derivatization would have led to either the absence of an unsaturated bond between atoms N(7) and C(8) or the presence of a positively charged N(7) quaternary ammonium moiety. The latter modification was already shown to be deleterious for nucleotide binding in previous studies [26]. Furthermore, because the entrance of the pocket was calculated to be rather narrow and because we wanted to allow some degree of conformational freedom for proper binding, we wished to introduce a flexible linker unit between the guanine ring and the hydrophobic head (Figure 2C).

Inhibitor Synthesis

Introduction of the carbon atom at position 7 was achieved by using C(7)-deazaguanine (**1**), prepared according to published procedures, as the starting material[27]. Briefly, C(7)-deazaguanine (**1**) was functionalized to permit

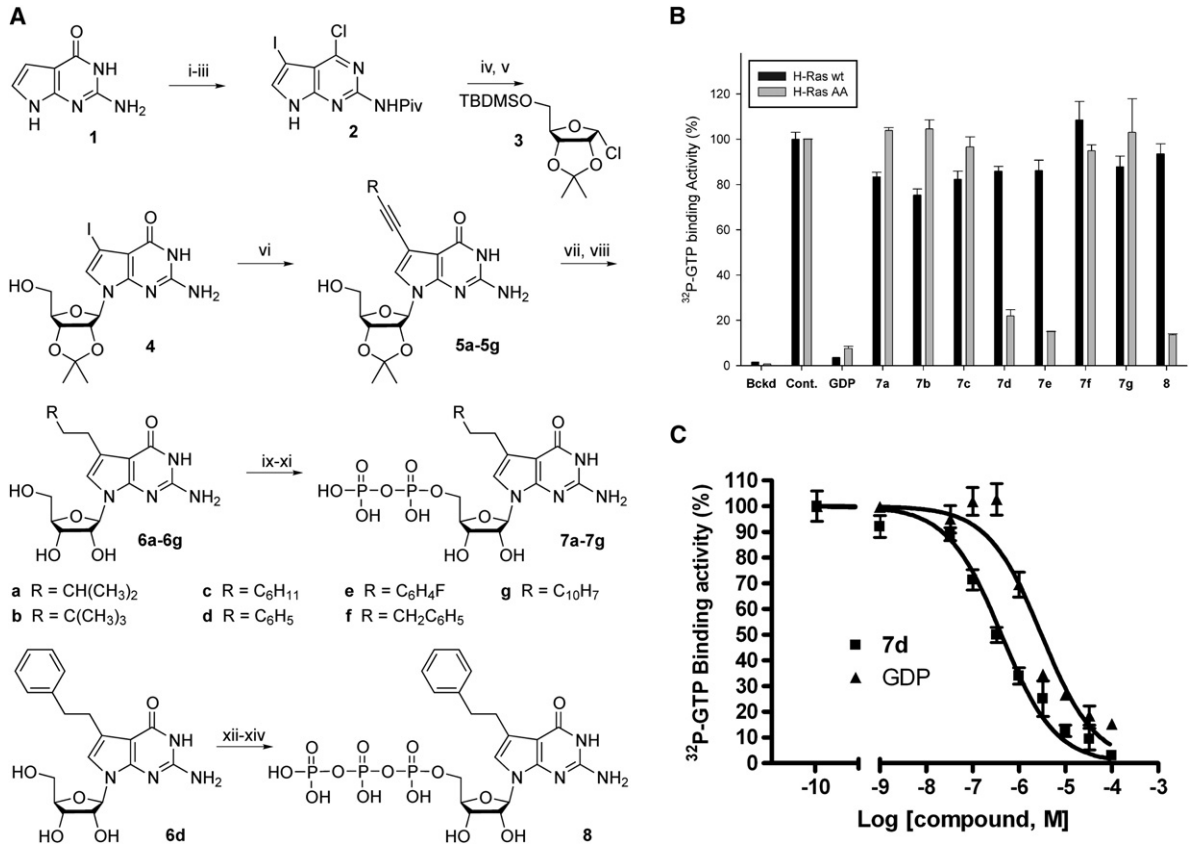

Figure 3. Synthesis and Binding Properties of Guanine Nucleotide Derivatives

(A) Conditions: (i) $POCl_3$, *N*, *N*-dimethylaniline, reflux, 3 hr, 79%; (ii) PivCl, pyridine, 1 hr, 62%; (iii) *N*-iodosuccinimide, THF, 1 hr, 86%; (iv) **3**, KOH, TDA, MeCN, 24 hr, 18%; (v) NaOH, dioxane, reflux, 4 hr, 71%; (vi) RC≡CH, $Pd(PPh_3)_4$, CuI, TEA, DMF, 4 hr, 72%–98%; (vii) H_2, Pd/C, 1–8 hr, 44%–97%; (viii) 70% aq.TFA, 1 hr, 65%–96%; (ix) $POCl_3$, trimethylphosphate, 0°C, 2 hr; (x) CDI, DMF, 24 hr; (xi) phosphoric acid, nBu_3N, MeOH-DMF, 7%–72% (over three steps); (xii) $POCl_3$, trimethylphosphate, 0°C, 2 hr; (xiii) CDI, DMF, 24 hr; (xiv) pyrophosphoric acid, nBu_3N, MeOH-DMF, 33% (over three steps).

(B) Comparison of the inhibition of [γ-^{32}P]GTP binding to H-Ras WT and AA enzymes by compounds **7a**–**7g** and **8** at 100 μM. The ability of [γ-^{32}P]GTP to displace inhibitors bound to the enzymes was measured by a filter binding assay. The enzymes were loaded with GDP, compounds **7a**–**7g** and **8**, or water (Cont.) as indicated. The background binding was determined in the absence of enzyme (Bckd).

(C) Comparison of the binding affinities of GDP and **7d** for H-Ras AA.

regioselective C(7) monoiodination to give compound **2** and thereby activate the C(7) position for further derivatization (Figure 3A). Additionally, the substitution pattern of **2** rendered it suitable for a stereoselective ribosylation at N(9) with activated sugar derivative **3**, made in situ with an Appel chlorination [28]. After a one-pot hydrolysis of the C(6) chloro, pivaloyl, and TBDMS moieties, acetonide-protected C(7)-deazaguanosine **4** was obtained. Subsequent Sonogashira Pd-mediated couplings with a variety of terminal alkynes afforded derivatives **5a**–**5g** [29]. Importantly, regio- and chemoselective reduction of the alkyne moiety could be achieved and was followed by deprotection of the C(2′) and C(3′) hydroxyls to yield compounds **6a**–**6g**. Finally, the C(5′) introduction of the two phosphate groups was done sequentially to afford GDP analogs **7a**–**7g** [17]. Triphosphate derivative **8** was prepared in a similar fashion by coupling first a single phosphate and then a pyrophosphate moiety to C(7)-deazaguanosine **6d**.

Nucleotide-Binding Specificities of WT and Mutant H-Ras

In order to create a variety of novel hydrophobic pockets, amino acids L19 and N116 were mutated to either alanine or glycine in all possible combinations. Overall, eight mutant H-Ras proteins were expressed as GST fusion proteins in *Escherichia coli* (19G-116N, 19A-116N, 19L-116G, 19L-116A, 19A-116A, 19G-116G, 19G-116A, and 19A-116G). The library of analogs was screened against both WT and mutant H-Ras enzymes by using a filter binding assay measuring the competitive displacement of the compounds by radiolabeled GTP [30]. Compounds possessing a substituted amine attached to C(6) or bearing large substituents at this position were unable to bind to the mutant proteins (data not shown). While compounds bearing an oxygen atom at C(6) and smaller substituents could inhibit some of the mutant enzymes, they also bound to H-Ras WT, and this lack of selectivity

disqualified them from further studies (data not shown). H-Ras 19A-116A (H-Ras AA) displayed the most promising results of all mutant enzymes for the C(7)-deazaguanine series of inhibitors (Figure 3B). While compounds **7a**–**7g** did not inhibit H-Ras WT, derivatives **7d** and **7e** efficiently prevented nucleotide exchange in H-Ras AA. Clear structure-activity relationships were apparent from these results. First, an unsaturated (planar) hydrophobic head was required for binding, as **7a**–**7c** were inactive. Second, the two-methylene linker unit was found to be necessary, as **7f** did not bind to the enzyme. Finally, modifications on the aromatic ring revealed that a small para substitution (**7e**) could be tolerated, while fusing another ring was not (**7g**). After confirming the binding selectivity of **7d**, its affinity was then compared to that of GDP (Figure 3C). Interestingly, **7d** was less easily displaced by [γ-^{32}P]GTP than GDP itself, exhibiting ~5-fold greater affinity for the mutant enzyme. This result indicated that the most demanding criterion, potency of the compounds versus the endogenous substrates, had been satisfied.

Tight binding of several GDP derivatives to H-Ras AA appeared to confirm that their binding mode was likely similar to that of GDP itself. Accordingly, this possibility strengthened our original prediction that the triphosphate equivalent of **7d**, compound **8**, might be a specific activator of H-Ras AA. After its synthesis, **8** was tested for its ability to prevent GTP binding to both H-Ras WT and H-Ras AA (Figure 3B). Specific binding of **8** to H-Ras AA was observed (Figure 3B), further implying that the binding mode of compounds **7d** and **8** might be analogous to that of GDP and GTP, respectively.

Characterization of Orthogonal Pairs H-Ras AA-7d and H-Ras AA-8

Once the selectivity and potency of **7d** and **8** were determined, we then investigated the ability of H-Ras AA to induce signaling in vitro and in a cellular context. Previous reports have documented the use of the GST-tagged Ras-binding domain (RBD) of Raf1 kinase in selectively pulling down GTP-loaded Ras to quantify Ras activation [31, 32]. We used this experimental setup to verify whether the engineered protein would still function properly as a "switch." H-Ras WT and H-Ras AA were loaded with GDP, GTP, **7d**, or **8** and incubated with GST-RBD attached to glutathione Sepharose beads. The unbound H-Ras was removed during the washing steps, allowing for the quantitation of protein bound (active Ras) to RBD by anti-Ras immunoblotting. As expected, minimal protein was observed for GDP-loaded, compared to GTP-loaded, H-Ras WT (Figure 4A, lane 1 versus lane 2) [32]. A similar pattern was visible for H-Ras AA (lane 3 versus lane 4). Furthermore, the inactivating effect of **7d** binding was illustrated by the low amount of mutant protein observed binding to RBD (lane 5). Interestingly, H-Ras AA loaded with triphosphate derivative **8** bound to RBD as well as when GTP was employed (lane 6 versus lane 4), thus indicating that **8** cannot only selectively bind to but also activate the mutant enzyme. H-Ras WT did not show any binding with either **7d** or **8**, as expected (Figure 4B). Overall, these results demonstrate that the engineered H-Ras conserves the ability to bind an effector selectively in the presence of GTP and, implicitly, to transmit signals. More importantly, compounds **8** and **7d** can turn it "on" and "off," respectively.

While H-Ras AA was demonstrated to retain its nucleotide- and effector-binding abilities in vitro, we sought both in vitro and in vivo confirmation of the functional innocuousness of the mutations chosen. This criterion for conformation was that the mutant protein should not only bind the same effectors, but also respond to the "on/off" switch mechanism as precisely as the WT enzyme. First, we investigated the interactions of H-Ras with the macromolecules that directly regulate its activity: a GEF (cdc25) and a GAP (RasGAP). The rate of background nucleotide exchange is identical for both H-Ras WT and H-Ras AA (Figure 4C). More importantly, the presence of cdc25 enhances the exchange rate to the same extent in each case (Figure 4C). Similar results were observed when GTP hydrolysis rates were analyzed in the presence and absence of RasGAP (Figure 4D). Based on these experiments, it can be concluded that the mutations introduced did not affect the interaction of H-Ras with the proteins regulating its activation status. Since H-Ras is known to induce transformation when overexpressed in NIH 3T3 fibroblasts [33], we established clonal cell lines expressing either H-Ras WT or H-Ras AA to compare their phenotypes. H-Ras AA-expressing NIH 3T3 cells were indistinguishable from the H-Ras WT-expressing cells, when Ras was present in comparable amounts (Figure 4E). Additionally, a proliferation assay was conducted to quantify the transformation abilities of either protein (Figure 4F). While few colonies were observed in the absence of any overexpressed Ras protein in the soft agar assay, cell lines expressing either type displayed a similar number of colonies. Engineered H-Ras thus appears to retain the transforming abilities of its WT counterpart, demonstrating conservation of the functions necessary for this event in vivo.

Since H-Ras AA behaved like the WT enzyme in biochemical and cellular assays, we wished to further investigate its specific binding to orthogonal compounds **7d** and **8**. Using X-ray crystallography data [34] representing H-Ras WT bound to GDP (Figure 1B), we conducted a molecular modeling study to scrutinize the binding of inhibitor **7d** to H-Ras AA. The tight affinities displayed by **7d** and **8** and their ability to control the conformational changes dictating association with effectors such as Raf1 kinase strongly suggested that their binding modes were similar to that of GDP and GTP, respectively. Interestingly, a stochastic search revealed the existence of a unique allowed conformation for the insertion of the aromatic ring into the newly created hydrophobic pocket (Figure 4G). The conformational freedom afforded by the two-methylene linker is clearly necessary for the proper localization of the ring. The additional binding affinity resulting from these novel hydrophobic interactions offers a reasonable explanation for the enhanced affinity of nucleotide **7d** versus GDP for the engineered enzyme.

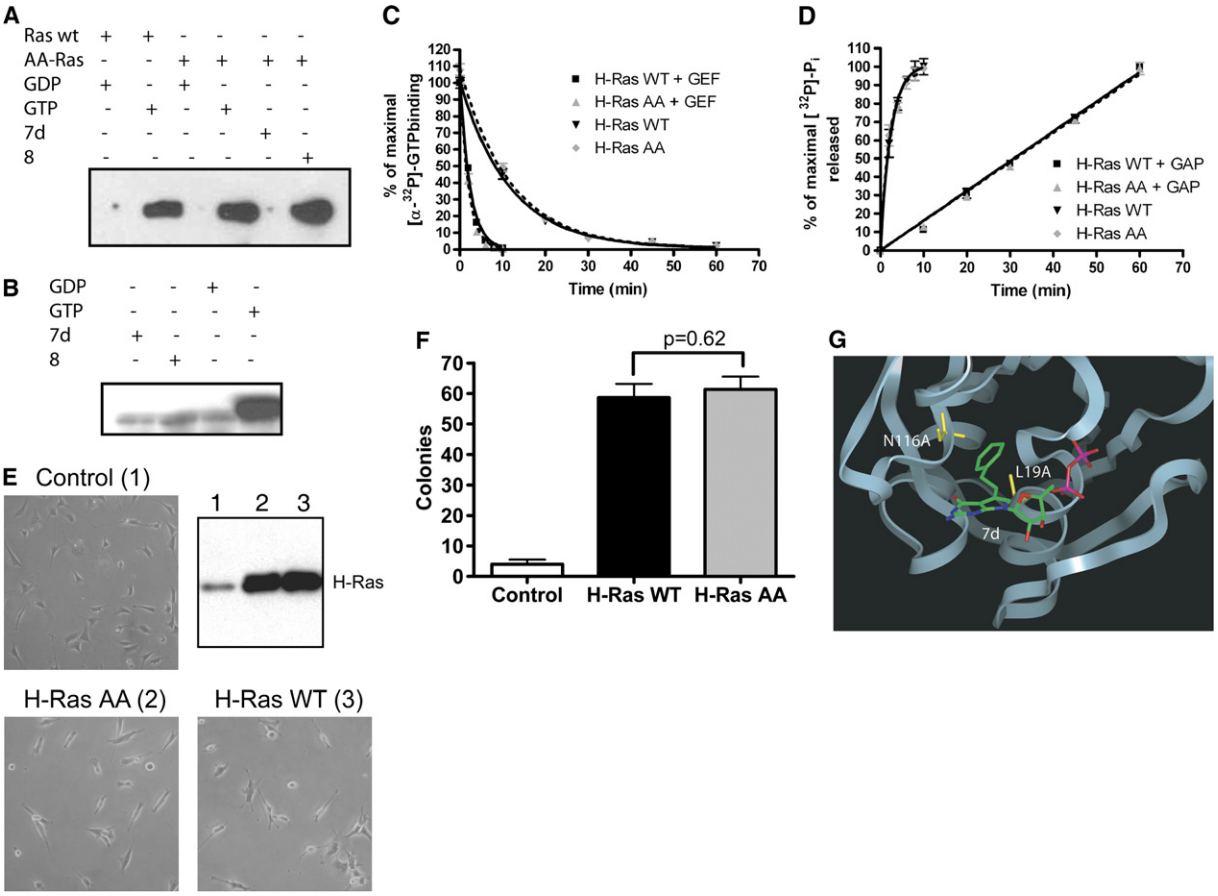

Figure 4. Characterization of H-Ras AA and of Its Interactions with Compounds 7d and 8

(A) Pull-down of H-Ras with GST-RBD bound to glutathione Sepharose beads. The amount of H-Ras WT (WT) or H-Ras AA (AA) pulled down by GST-RBD in the presence of GDP (lanes 1 and 3), GTP (lanes 2 and 4), **7d** (lane 5), and **8** (lane 6) is shown by anti-Ras immunobloting.

(B) Pull-down of H-Ras WT with GST-RBD bound to glutathione beads with compound **7d** (lane 1), **8** (lane 2), GDP (lane 3), and GTP (lane 4).

(C) Amount of exchanged GTP as a function of time for H-Ras WT and H-Ras AA in the absence and presence of cdc25c.

(D) Amount of hydrolyzed GTP (Pi) as a function of time for H-Ras WT and H-Ras AA in the absence and presence of RasGAP.

(E) Transformation of NIH 3T3 fibroblasts by H-Ras WT and H-Ras AA. Clonal cell lines isolated from NIH 3T3 fibroblasts infected with retroviruses containing H-Ras WT and H-Ras AA are shown. H-Ras levels are shown in the insert: (1) Control, (2) H-Ras WT, and (3) H-Ras AA.

(F) Number of colonies counted in a soft agar assay conducted with the clonal cell lines described above. The p value displayed was obtained from a two-tailed t test.

(G) Ribbon representation of the proposed binding mode of **7d** to H-Ras AA; **7d** docking was conducted by using the modeling software MOE, and the output was visualized with Insight II.

Selective Identification of G Protein Effectors

We expanded this approach further to identify, in a specific, unbiased manner, novel H-Ras effectors in complex biological samples. GST-tagged H-Ras AA molecules bound to glutathione Sepharose beads were loaded with triphosphate **8** for activation. A cell lysate, dialyzed against a saline solution containing both EDTA and GDP, was then added to the H-Ras AA beads in the presence of excess magnesium, a necessary cofactor for tight nucleotide binding [22]. H-Ras AA was activated and able to bind its downstream effectors. As multiple members of the Ras family can bind to the same effectors [34], this specificity of activation prevents the competition of H-Ras AA with multiple G proteins for the same set of effectors. After washings aimed at removing unbound proteins, the beads were treated with excess EDTA and GDP to loosen the binding of **8** to H-Ras AA and to ensure its replacement by GDP [26]. As a result, conformational changes of H-Ras AA led to the selective release of the bound effectors under mild conditions (Figure 5A, lane 2), while proteins binding unspecifically to the beads were retained. The addition of controls such as "blank" elution (no EDTA or GDP) of an identical sample (lane 1) or the elution of proteins binding to GDP-loaded H-Ras AA (lane 3) allows for the further elimination of background signal. As a positive control, we monitored the amount of Raf kinase, a known H-Ras effector, present in the different elution fractions. Figure 5B documents the presence of Raf in the specific elution fraction (lane 2), while none was found in the two control samples (lanes 1 and 3). Furthermore, similar experiments

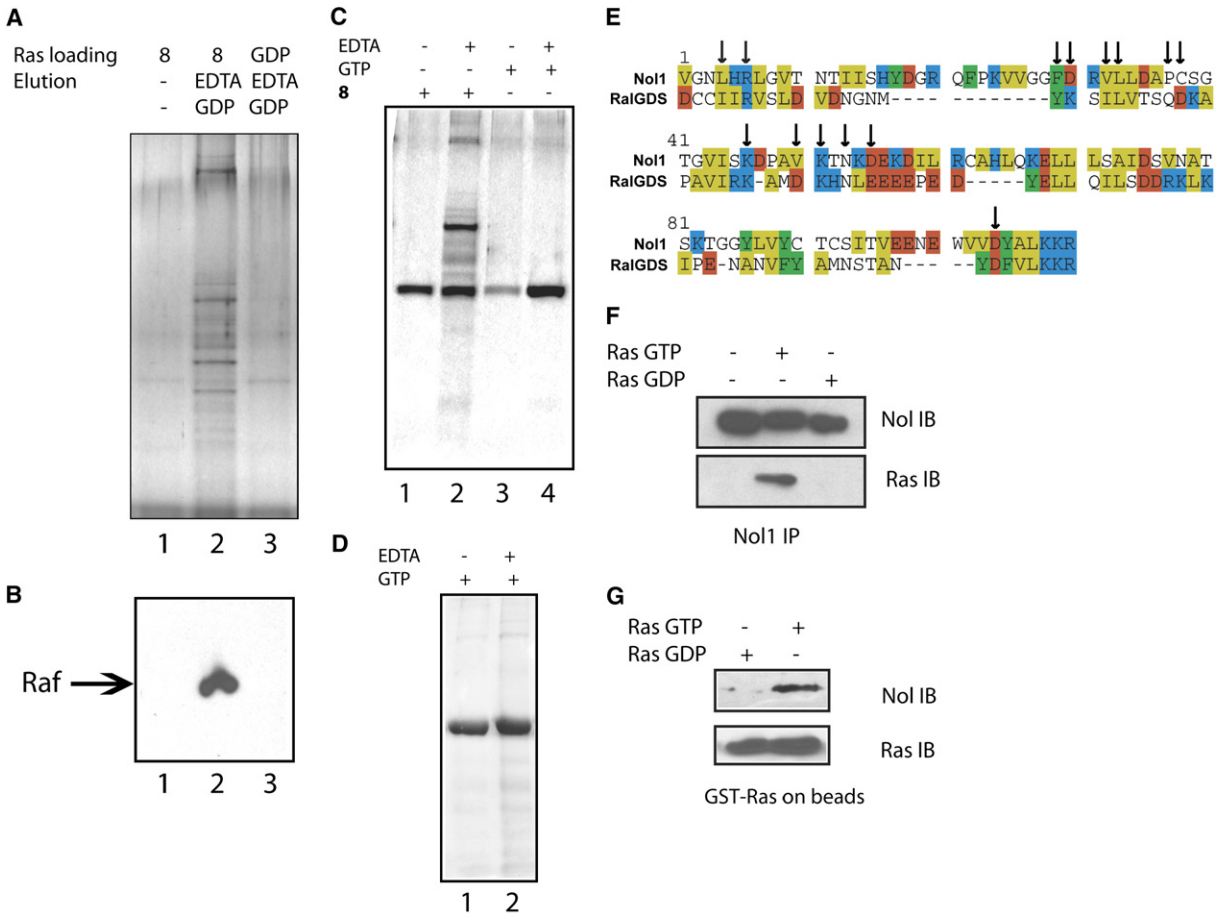

Figure 5. Selective Isolation of H-Ras Effectors

(A) Silver-stained gel displaying the proteins isolated from whole-cell lysate by GST-H-Ras AA activated with **8** (10 μM, samples 1 and 2) or inactivated with GDP (10 μM, sample 3) and eluted with EDTA and GDP (lanes 2 and 3) or buffer without EDTA or GDP (lane 1) as described in Experimental Procedures. Proteins uniquely present in lane 2 associated with activated H-Ras AA and were specifically released after H-Ras AA inactivation and are therefore candidate effectors of H-Ras.

(B) Anti-Raf1 immunoblot of the same experiment displaying Raf protein eluted from samples 1–3.

(C) Silver-stained gel displaying the proteins isolated from whole-cell lysate by GST-H-Ras AA activated with **8** (10 μM, samples 1 and 2) or with GTP (10 μM, samples 3 and 4) and eluted with EDTA and GDP (lanes 2 and 4) or buffer without EDTA or GDP (lane 1 and 3) as described in Experimental Procedures.

(D) GST-H-Ras activated with GTP (10 μM) and eluted with buffer only (lane 1) or with buffer supplemented with EDTA and GDP (lane 2).

(E) Sequence alignment of human Nol1 (accession number P46087, amino acids 425–535) with the RA domain of human Ral-GDS (accession number Q12967, amino acids 798–883). Alignment was produced by using ClustalW and was manually refined and colored by using Seaview (red, negatively charged; blue, positively charged; green, aromatic; yellow, lipophilic amino acids). Arrows indicate amino acids important in the binding of RalGDS to H-Ras.

(F) Nol1 immune complexes incubated with no protein, Ras-GTP, or Ras-GDP were immunoblotted for Nol1 and Ras.

(G) GST-Ras on glutathione beads loaded with GDP (lane 1) or GTP (lane 2) were incubated with MCF7 cell lysates as described in Experimental Procedures. Nol1 IB shows specific binding upon Ras activation (lane 2).

comparing GTP with compound **8** led to higher levels of isolated proteins with the latter (Figure 5C, compare lanes 2 and 4). Presumably, this effect may stem from the fact that all G proteins should be activated by GTP. Similar results were obtained when WT Ras was used with GTP, showing minimal effectors (Figure 5D). The protocol developed thus permits the specific isolation and identification of novel effectors of G proteins on a proteome-wide scale. Two-dimensional gel electrophoresis can then be used for the resolution of individual proteins and mass spectrometry for their identification. An important feature of this method is the large enrichment in effector proteins due to the specific binding and elution procedures with a mild EDTA-mediated release mechanism that favors elution of the proteins specifically bound to activated H-Ras.

Proposal of Nol1 as a Putative Novel Effector of Ras

Using the approach outlined above, Nol1 (proliferating cell nucleolar protein p120) was suggested as a putative

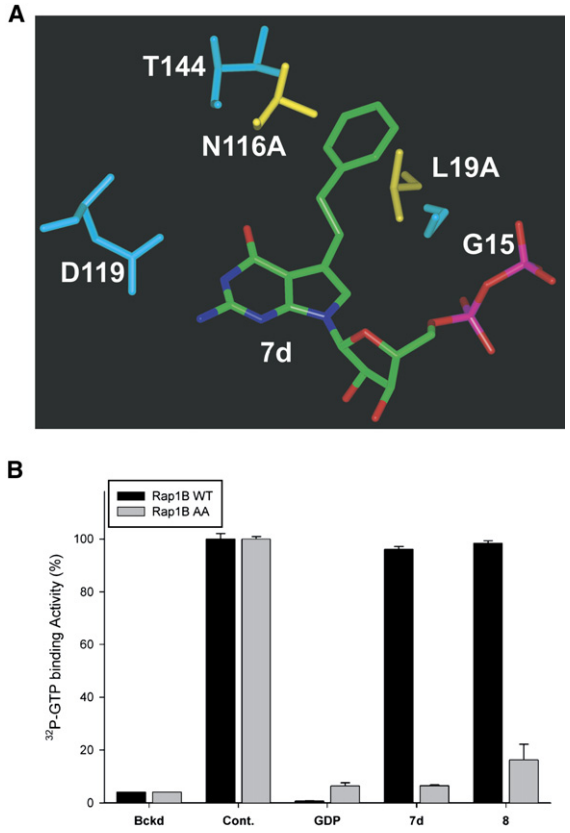

Figure 6. System Transfer to Other G Proteins

(A) Close-up view of **7d** inside the modified active site; important amino acids are depicted.

(B) Comparison of the inhibition of [γ-^{32}P]GTP binding to Rap1B WT and AA enzymes by compounds **7d** and **8** at 100 μM. The ability of [γ-^{32}P]GTP to displace inhibitors bound to the enzymes was measured by a filter binding assay. The enzymes were loaded with GDP, compounds **7d** and **8**, or water (Cont.) as indicated. The background binding was determined in the absence of enzyme (Bckd).

binding partner of H-Ras AA by mass spectroscopy. Two consensus sequences have been identified for Ras effectors to date—RBD and RA (Ras association) domain—although not all proteins bearing RA domains identified through sequence alignments are genuine Ras effectors [35]. No RBD or RA domains are predicted to exist in Nol1 according to the SMART and PFAM databases [36, 37]. Interestingly, while the alignment of Nol1 with the RBD of Raf was unsuccessful, significant overlap (~17% identity) was observed with the RA domain of RalGDS (Figure 5E), another well-characterized effector of Ras. Furthermore, a number of the amino acids depicted as important in the binding of RalGDS to Ras appear to be preserved [35, 38].

To confirm that Nol1 can bind to H-Ras, Nol1 immune complexes were isolated from MCF7 cells and incubated with H-Ras WT preloaded with either GTP or GDP. Nol1 specifically bound to the active form (lane 2), but not to the inactive form (lane 3), of Ras (Figure 5F). Additionally, GST-Ras (on beads) preloaded with either GTP or GDP was added to MCF7 cell lysates, and Nol1 binding was probed. Nol1 binds to active Ras specifically (Figure 5G). This result suggests that Nol1 may be a novel effector of H-Ras.

System Transfer to Other G Proteins

In the design phase of this study, great emphasis was placed on the potential transferability of the designed orthogonal small-molecule/protein pairs to other G proteins. The overall fold of the guanine nucleotide-binding domain of G proteins has been studied previously and was found to be conserved across all subfamilies, resulting in substantial amino acid identity in residues located near the active site [22]. Investigation of the engineered hydrophobic pocket highlighted the pivotal role of threonine 144 (T144) in allowing for the presence of the phenyl ring inside the pocket (Figure 6A). As the aromatic ring nestles between L19A and N116A, this is the closest nonconserved amino acid. Its identity can thus be potentially crucial in allowing or disrupting the binding of compounds **7d** and **8** to a given engineered G protein. Due to the conserved hydrogen bond between the amide nitrogen of A146 and O(6), the orientation of T144 inside the pocket is well preserved in G proteins. Interestingly, sequence alignments reveal that this position is occupied in the vast majority of cases by similar amino acids such as cysteine or serine (Figure 2A).

Rap1 proteins are implicated in growth and differentiation modulation, secretion, cell adhesion, and morphogenesis [34]. Sequence alignments indicated the conservation of L19 and N116, and thus these residues were targeted for alanine mutations. Importantly, the other key residue, T144 in H-Ras, corresponds to S146 (Figure 2). Rap1B thus provided an opportunity to test our compounds with a different amino acid at this position and validate the strategy used for creating inhibitor **7d** and activator **8**, which are specific for the G protein family. A binding assay with both Rap1B WT and Rap1B AA in conjunction with GDP, **7d**, or **8** was then carried out. Results displayed the selective binding of derivatives **7d** and **8** to the engineered Rap1B enzyme only (Figure 6B), further illustrating the potential for straightforward adaptation of the orthogonal small-molecule/G protein pairs crafted in this study to any G protein of interest.

DISCUSSION

The importance of Ras proteins as crucial players at the crossroads in cellular signaling pathways is well established [7]. However, the overall framework of Ras interactions is far from complete, and the collection of Ras effectors continues to expand, uncovering links between Ras and other cellular signaling pathways. Ras is emerging as a dual regulator of cellular functions, playing either positive or negative roles in the regulation of proliferation and apoptosis [38]. Characteristics of G proteins, such as picomolar binding affinities for GDP and GTP, have precluded the development or the isolation of active-site-directed inhibitors or activators. To answer this need, we

envisioned an approach allowing for the specific modulation of H-Ras activity that could then easily be applied to other G proteins. This tool could thus be used for deciphering individual G protein signaling cascades through the tight "on" and "off" control afforded by small molecules and the specific isolation of G protein-binding partners. To accomplish this, an additional binding pocket was engineered into the guanine nucleotide-binding site (Figure 2), and GDP/GTP derivatives bearing bulky substituents were synthesized to complement these mutations (Figure 3A). Compound **7d** was observed to bind selectively and potently to H-Ras AA, resulting in the inhibition of its activity (Figures 3B, 3C, and 4A). In contrast, triphosphate analog **8** specifically activated H-Ras AA, as observed by using the RBD pull-down (Figures 4A and 4B). Conservation of the functions of the engineered H-Ras was first demonstrated by its preserved ability to bind GDP and GTP (Figures 3B and 3C). Second, GDP and GTP were confirmed to induce conformational changes in the engineered protein similar to those produced in the WT enzyme (Figure 4A). Third, neither GEF-mediated nucleotide exchange nor GAP-stimulated GTP hydrolysis were found to be affected in the engineered protein (Figures 4C and 4D). Additionally, while most previously known H-Ras mutants, including xanthosine nucleotide-binding proteins, display either dominant-negative or constitutive activity properties in a cellular context [21], H-Ras AA behaved as its WT counterpart in NIH 3T3 fibroblasts (Figures 4E and 4F). Finally, we conducted modeling studies illustrating the potential for transfer of the system created, as the orthogonal inhibitor (**7d**) and activator (**8**) appeared to have the same binding mode as their natural counterparts (Figure 4G).

Importantly, since engineered H-Ras is functionally indistinguishable from H-Ras WT, this approach can be utilized for in vivo studies in different cell types. While nucleotide analogs are not cell permeable, whole-cell dialysis, microinjection, and cell permeabilization are effective techniques for small-molecule-based activation or inhibition to study cellular events. We reported recently the successful use of an ADP analog to delineate the role of myosin-1c in hair-cell adaptation in vivo [16]. Moreover, this chemical-genetic strategy is especially powerful, as it allows for negative controls not accessible by other methods, such as using H-Ras WT-expressing cells for filtering out the nonspecific effects of microinjection and other artifacts. These tools, in conjunction with the highly specific inhibition or activation of a desired G protein in the cell should thus enable us to study the role of G proteins implicated in cytoskeleton dynamics, cell-cycle progression, and nuclear transport, for example.

The diversity of Ras-mediated effects may be related, in part, to differential involvement of Ras homologs in distinct cellular processes [7]. Therefore, the identification of the specific effectors of Ras homologs in different cell types will significantly enrich our understanding of their individual functions [39]. To this aim, we utilized this chemical-genetic tool to uncover novel H-Ras effectors in whole-cell lysate. Through the selective activation of H-Ras AA by **8** and the specific EDTA- and GDP-mediated release, H-Ras effectors could be highly enriched in the final elution (Figures 5A and 5C). This approach offers a novel way to study any G protein through the identification of its binding partners.

We demonstrate the feasibility of this approach by identifying and proposing Nol1 as a putative novel effector of H-Ras (Figures 5E–5G). Hypothesized to be an RNA methyltransferase, Nol1 is expressed by cells in early G1 phase and peaks during S phase [40]. Multiple reports document its overexpression in a variety of tumors, including lung adenocarcinoma [41], prostate adenocarcinoma [42], breast cancer [43], oral carcinoma [44], follicular lymphoma [45], and human gliomas [46], and this overexpression is correlated with poor prognosis and shorter patient survival. Its expression levels in a wide range of human cancer cell lines were also found to be predictive of cellular doubling times [47]. Furthermore, expression of Nol1 in NIH 3T3 cells results in transformation and produces rapidly growing tumors in nude mice [48]. Identification of Nol1 as a possible downstream effector of Ras might thus suggest a novel mechanism by which Ras may influence carcinogenesis. Further research will be necessary to investigate the consequences of activated H-Ras binding to Nol1 in healthy or diseased tissue.

Finally, to ensure the transferability of this approach to other G proteins of interest, we demonstrated a straightforward transfer to Rap1B (Figure 6B). As understanding the precise functions of closely related family members is a current frontier in Ras research, this specific control over the activity of a given member is of particular interest [7]. More importantly, successful sensitization of a different G protein to the compounds controlling the activity of the previously engineered H-Ras demonstrates the potential breadth of application of this approach.

SIGNIFICANCE

In conclusion, we demonstrate the structure-based design of complementary small-molecule/protein pairs for H-Ras. The strategy employed allows for the selective inhibition and activation of an engineered H-Ras mutant by two related compounds. The high degree of homology between nucleotide-binding sites and the conservation of the residues targeted for mutation suggests that other members of the family can be successfully sensitized to the action of modulators 7d and 8. Indeed, the approach was generalized to an additional G protein, Rap1B. Its application further led to the proposal of Nol1 as a putative novel H-Ras effector. Due to its absolute selectivity, this chemical-genetic approach should be a valuable addition to researchers' toolkits for the functional study of individual members of the G protein family.

EXPERIMENTAL PROCEDURES

Cloning and Expression of H-Ras and Rap1B Mutants

The mutant human *H-Ras* protein constructs were created in the pGEX-4T1 vector by using the QuikChange protocol (Stratagene). A

single colony was inoculated into 10 ml LB superbroth media with 50 μg/ml carbenicillin and was grown at 37°C overnight. This culture was added to 500 ml LB superbroth. After it had grown to an OD of ~0.6, protein synthesis was induced by IPTG (50 μM) and by further shaking at 30°C for 12 hr. After centrifugation at 3,500 × g for 15 min at 4°C, the cell pellet was frozen at −80°C for 1 hr. The pellet was resuspended in chilled lysis buffer (20 mM HEPES [pH 7.5], 75 mM KCl, 25 mM $MgCl_2$, 5 mM DTT, 0.1 mM EDTA, 0.05% Triton X-100, and protease inhibitors [Sigma]) and was further sonicated for 60 s. The resulting lysate was centrifuged at 30,000 × g for 30 min at 4C, and the supernatant was added to glutathione Sepharose beads and was incubated at 4°C with rotation. The beads were washed with lysis buffer once, then with wash buffer (50 mM Tris-HCl [pH 7.5], 50 mM NaCl, 1 mM DTT) three times. The protein was eluted with 10 mM glutathione in wash buffer, concentrated, and dialyzed overnight against storage buffer (50 mM Tris-HCl [pH 7.5], 50 mM NaCl, 0.2 mM DTT, 0.1 mM EDTA). Protein concentration was determined by a Bradford assay, and the protein purity was assessed by gel electrophoresis.

Guanine Nucleotide Exchange Assays

The purified proteins (inhibitor screening: 5 μg; affinity curve: 300 ng) were incubated in 40 μl of GTP exchange buffer (50 mM Tris-HCl [pH 7.5], 50 mM NaCl, 0.5 mM $MgCl_2$, 1 mM DTT, 1 mg/ml BSA) containing either water, GDP (100 μM) or an inhibitor (100 μM) for 30 min at 25°C. This preincubation was followed by the addition of GTP (10 nM) containing 2 μCi [γ-^{32}P]GTP (NEN) with 25 mM $MgCl_2$. After another 5 min of incubation, the reaction mixture was applied to a nitrocellulose filter (Millipore) prewetted with wash buffer (50 mM Tris-HCl [pH 7.5], 10 mM $MgCl_2$), and the filter was then washed with 10 ml wash buffer. Filters were dried, and the bound radioactivity was measured by scintillation counting.

RBD Pull-Down Assay

The purified proteins (150 ng) were incubated in 1 ml of loading buffer (100 mM Tris-HCl [pH 7.5], 2 mM EDTA, 1 mM DTT, 1 mg/ml BSA) in the presence of 10 μM GDP, GTP, **7d**, or **8** for 15 min at 25°C for loading the proteins with the appropriate nucleotides. After loading, $MgCl_2$ (20 mM) was added along with GST-RBD (1.2 μg), comprising Raf kinase amino acids 53–131, bound to glutathione Sepharose beads. The resulting suspensions were incubated with rotation for 15 min at 4°C. The beads were then washed three times with 1 ml washing buffer (50 mM Tris-HCl [pH 7.5], 100 mM NaCl, 20 mM $MgCl_2$, 1 mM DTT) and boiled in SDS loading buffer, and the samples were separated by electrophoresis. After transfer, the PVDF membrane was probed with anti-H-Ras (Santa Cruz, C-20), and the amount of H-Ras bound to the RBD glutathione Sepharose beads was visualized by using anti-rabbit HRP in conjunction with West Pico (Pierce).

Nol-1 Pull-Down Assay

Nol-1 immune complexes (Protein Tech Group, Chicago) isolated from MCF7 cells were incubated with GST-Ras (1 μg each) preloaded with either GTP or GDP as described above. The resulting suspensions were incubated with rotation for 20 min at 4°C. The beads were then washed three times with 1 ml of washing buffer as described above, boiled in SDS loading buffer, and separated by electrophoresis. After transfer, the PVDF membrane was probed with anti-H-Ras and anti-Nol1 (for loading control), followed by anti-rabbit HRP in conjunction with West Pico (Pierce).

Alternatively, GST-Ras on glutathione beads (1 μg each) preloaded with either GTP or GDP was incubated with MCF7 cell lysates with rotation for 20 min at 4°C in the presence of GTP or GDP (10 μM). The beads were washed, boiled, separated, and transferred as described above. The PVDF membrane was probed with anti-Nol1 and anti-Ras (for loading control).

GAP-Mediated Nucleotide Hydrolysis Assay

A total of 5 μg of either H-Ras or H-Ras AA protein was incubated with 5 μM GTP and 2 μCi [γ-^{32}P]GTP in GTPase reaction buffer at 30°C (20 mM Tris-HCl [pH 7.5], 100 mM NaCl, 1 mM DTT) in triplicate in a total assay volume of 350 μl. After 10 min, $MgCl_2$ was added at a final concentration of 25 mM. Samples (50 μl) were collected at different times (starting from t = 0–60 min), and the reaction was stopped by adding 750 μl 5% w/v activated charcoal in 20 mM ice-cold phosphoric acid and centrifuging for 10 min. Radioactivity was quantified by liquid scintillation counting of 500 μl of the supernatants containing hydrolyzed $^{32}P_i$. For tubes containing GAP, 5 μg of GST-GAP was added after the preloading step, and samples were collected at 2 min intervals up to 10 min.

GEF-Mediated Nucleotide Exchange Assay

A total of 5 μg of either H-Ras or H-Ras AA was preloaded with 1 μM GTP and 5 μCi [α-^{32}P]GTP in loading buffer in triplicate (20 mM Tris [pH 7.5], 100 mM NaCl, 1 mM DTT) at 30°C in a total volume of 350 μl. After 40 min, GTP was added at a final concentration of 100 μM loading buffer (50 μl). Samples (50 μl) were collected and added to 1 ml ice-cold stop buffer (50 mM Tris-HCl [pH 7.5], 20 mM $MgCl_2$, 1 mM DTT, 10 μg/ml BSA) at regular intervals (starting at t = 0 up to 60 min). The resulting mixture was filtered through prewetted nitrocellulose filters (0.45 μm, white grided HAWG, 25 mm) under vacuum and washed with 10 ml wash buffer (50 mM Tris-HCl [pH 7.5], 10 mM $MgCl_2$). Radioactivity was quantified by liquid scintillation counting after drying the filters. For tubes containing GEF, 1 μg cdc25c was included in the reaction mixture after the preloading step, and samples were collected at 2 min intervals up to 10 min.

Transforming Abilities of H-Ras WT and H-Ras AA

NIH 3T3 cells were cultured in DMEM supplemented with 10% bovine calf serum. *H-Ras WT* and *H-Ras AA* were cloned into pBabe puro and transfected into Bosc23 cells to produce virus. Pools of transduced rodent fibroblasts were selected by addition of puromycin (2.5 μg/ml). Clonal cells were isolated and grown under selection for 2 weeks. Cells displaying similar amounts of H-Ras WT and H-Ras AA by anti-H-Ras immunoblotting were chosen for further studies.

Soft-Agar Colony Formation Assay

Wild-type and H-Ras AA-expressing NIH 3T3 cells and pBabe vector-infected NIH 3T3 cells were plated in DMEM (10^3, 10^4, and 10^5 cells per dish, each in triplicate), 0.3% agar, and 10% calf serum in 35 × 10 mm dishes. Transformed colonies were counted after 3 weeks.

Molecular Modeling

Using PDB entry 1Q21 as a template, docking of **7d** to H-Ras AA was accomplished by using MOE (Chemical Computing Group). Briefly, amino acids L19 and N116 were mutated to alanine residues. The resulting structure (bound to GDP) was then energy minimized. After modifying GDP into **7d**, all atoms of the protein/nucleotide complex were fixed, except for those that were part of the added 1-ethylphenyl unit. A stochastic conformational search was run for these atoms, and a unique favorable conformation was obtained. This confirmation was further energy minimized, and the output was visualized with Insight II (Accelrys).

Selective Isolation of H-Ras Effectors

The HeLa cell pellet obtained from 15 × 150 mm plates was lysed using 10 mM Tris (pH 7.5), 150 mM NaCl, 1% NP40, 2 mM EDTA, GDP 100 μM, protease inhibitors (Sigma), and phosphatase inhibitors (Sigma cocktail I). After its centrifugation, the lysate (4.5 ml) was dialyzed against 10 mM Tris (pH 7.5), 50 mM NaCl, 0.1 mM EDTA for 4 hr at 4°C. Cell lysis in the presence of EDTA and GDP ensured that all cellular G proteins were loaded with GDP, while dialysis removed excess EDTA and GDP. The lysate was then precleared with 200 μl glutathione Sepharose beads for 30 min at 4°C. Engineered H-Ras AA (~20 μg) was immobilized on glutathione Sepharose beads

(50 μl) and was loaded with triphosphate derivative **8** (150 μM, tubes 1 and 2) or with GDP (150 μM, tube 3) during an incubation (15 min, 20°C) in 100 μl 10 mM Tris (pH 7.5), 50 mM NaCl, 0.1 mM EDTA. After addition of $MgCl_2$ (10 mM) to both beads in tubes 1–3 and dialyzed lysate, 1.4 ml lysate was added to each tube, and incubation was conducted at 4°C for 15 min with a final nucleotide concentration of 10 μM in each tube. The beads were then washed three times with 1 ml wash buffer A (10 mM Tris [pH 7.5], 100 mM NaCl, 10 mM $MgCl_2$, 1 μM **8**) for tubes 1 and 2 or wash buffer B (10 mM Tris [pH 7.5], 100 mM NaCl, 10 mM $MgCl_2$, 1 μM GDP) for tube 3. The elution was then conducted at 4°C for 30 min by adding 60 μl elution buffer A (10 mM Tris [pH 7.5], 30 mM NaCl, 10 mM $MgCl_2$, 1 μM **8**) to tube 1 (blank elution) or elution buffer B (10 mM Tris [pH 7.5], 30 mM NaCl, 20 mM EDTA, 100 μM GDP) to tubes 2 and 3. The supernatant was mixed with SDS loading buffer and boiled, and the proteins were separated by gel electrophoresis. The first gel was stained with silver stain to visualize the eluted proteins, while the other gel was transferred onto a PVDF membrane. The membrane was probed with anti-Raf1 (Santa Cruz Biotechnology, C-12), and the amount of Raf1 kinase present in each lane was visualized with anti-rabbit HRP in conjunction with West Pico (Pierce).

Supplemental Data

Supplemental Data include synthetic procedures and characterization data for key compounds and are available at http://www.chembiol.com/cgi/content/full/14/9/1007/DC1/.

ACKNOWLEDGMENTS

This work was funded by Genomics Institute of the Novartis Research Foundation and Walther Cancer Institute. We wish to thank Yi Liu and Oleksandr Buzko for help with molecular modeling, and Lawrence Quilliam for cdc25c and RasGAP cDNAs. The authors declare that they have no competing financial interests.

Received: June 29, 2007
Revised: July 23, 2007
Accepted: August 1, 2007
Published: September 21, 2007

REFERENCES

1. Venter, J.C., Adams, M.D., Myers, E.W., Li, P.W., Mural, R.J., Sutton, G.G., Smith, H.O., Yandell, M., Evans, C.A., Holt, R.A., et al. (2001). The sequence of the human genome. Science *291*, 1304–1351.
2. Vetter, I.R., and Wittinghofer, A. (2001). The guanine nucleotide-binding switch in three dimensions. Science *294*, 1299–1304.
3. Benard, V., Bokoch, G.M., and Diebold, B.A. (1999). Potential drug targets: small GTPases that regulate leukocyte function. Trends Pharmacol. Sci. *20*, 365–370.
4. Boquet, P., Sansonetti, P.J., and Tran Van Nhieu, G. (1999). Rho GTP-binding proteins as targets for microbial pathogens. Prog. Mol. Subcell. Biol. *22*, 183–199.
5. de Gunzburg, J. (1999). Proteins of the Ras pathway as novel potential anticancer therapeutic targets. Cell Biol. Toxicol. *15*, 345–358.
6. Downward, J. (2003). Targeting RAS signalling pathways in cancer therapy. Nat. Rev. Cancer *3*, 11–22.
7. Malumbres, M., and Barbacid, M. (2003). Ras oncogenes: the first 30 years. Nat. Rev. Cancer *3*, 7–13.
8. Hunter, T. (2000). Signalling–2000 and beyond. Cell *100*, 113–127.
9. Bishop, A., Buzko, O., Heyeck-Dumas, S., Jung, I., Kraybill, B., Liu, Y., Shah, K., Ulrich, S., Witucki, L., Yang, F., et al. (2000). Unnatural ligands for engineered proteins: new tools for chemical genetics. Annu. Rev. Biophys. Biomol. Struct. *29*, 577–606.
10. Coward, P., Wada, H.G., Falk, M.S., Chan, S.D., Meng, F., Akil, H., Conklin, B.R., et al. (1998). Controlling signaling with a specifically designed Gi-coupled receptor. Proc. Natl. Acad. Sci. USA *95*, 352–357.
11. Peet, D.J., Doyle, D.F., Corey, D.R., and Mangelsdorf, D.J. (1998). Engineering novel specificities for ligand-activated transcription in the nuclear hormone receptor RXR. Chem. Biol. *5*, 13–21.
12. Lin, Q., Jiang, F., Schultz, P.G., and Gray, N.S. (2001). Design of allele-specific protein methyltransferase inhibitors. J. Am. Chem. Soc. *123*, 11608–11613.
13. Klemm, J.D., Schreiber, S.L., and Crabtree, G.R. (1998). Dimerization as a regulatory mechanism in signal transduction. Annu. Rev. Immunol. *16*, 569–592.
14. Shah, K., Liu, Y., Deirmengian, C., and Shokat, K.M. (1997). Engineering unnatural nucleotide specificity for Rous sarcoma virus tyrosine kinase to uniquely label its direct substrates. Proc. Natl. Acad. Sci. USA *94*, 3565–3570.
15. Bishop, A.C., Ubersax, J.A., Petsch, D.T., Matheos, D.P., Gray, N.S., Blethrow, J., Shimizu, E., Tsien, J.Z., Schultz, P.G., Rose, M.D., et al. (2000). A chemical switch for inhibitor-sensitive alleles of any protein kinase. Nature *407*, 395–401.
16. Holt, J.R., Gillespie, S.K., Provance, D.W., Shah, K., Shokat, K.M., Corey, D.P., Mercer, J.A., and Gillespie, P.G. (2002). A chemical-genetic strategy implicates myosin-1c in adaptation by hair cells. Cell *108*, 371–381.
17. Hwang, Y.W., and Miller, D.L. (1987). A mutation that alters the nucleotide specificity of elongation factor Tu, a GTP regulatory protein. J. Biol. Chem. *262*, 13081–13085.
18. Weijland, A., Parlato, G., and Parmeggiani, A. (1994). Elongation factor Tu D138N, a mutant with modified substrate specificity, as a tool to study energy consumption in protein biosynthesis. Biochemistry *33*, 10711–10717.
19. Chung, J.H., Back, J.H., Park, Y.I., and Han, Y.S. (2001). Biochemical characterization of a novel hypoxanthine/xanthine dNTP pyrophosphatase from *Methanococcus jannaschii*. Nucleic Acids Res. *29*, 3099–3107.
20. Lin, S., McLennan, A.G., Ying, K., Wang, Z., Gu, S., Jin, H., Wu, C., Liu, W., Yuan, Y., Tang, R., et al. (2001). Cloning, expression, and characterization of a human inosine triphosphate pyrophosphatase encoded by the itpa gene. J. Biol. Chem. *276*, 18695–18701.
21. Cool, R.H., Schmidt, G., Lenzen, C.U., Prinz, H., Vogt, D., and Wittinghofer, A. (1999). The Ras mutant D119N is both dominant negative and activated. Mol. Cell. Biol. *19*, 6297–6305.
22. Sprang, S.R. (1997). G protein mechanisms: insights from structural analysis. Annu. Rev. Biochem. *66*, 639–678.
23. Bourne, H.R., Sanders, D.A., and McCormick, F. (1991). The GTPase superfamily: conserved structure and molecular mechanism. Nature *349*, 117–127.
24. Colicelli, J. (2004). Human RAS superfamily proteins and related GTPases. Sci. STKE *250*, RE13.
25. Wittinghofer, F., Krengel, U., John, J., Kabsch, W., and Pai, E.F. (1991). Three-dimensional structure of p21 in the active conformation and analysis of an oncogenic mutant. Environ. Health Perspect. *93*, 11–15.
26. Rensland, H., John, J., Linke, R., Simon, I., Schlichting, I., Wittinghofer, A., and Goody, R.S. (1995). Substrate and product structural requirements for binding of nucleotides to H-ras p21: the mechanism of discrimination between guanosine and adenosine nucleotides. Biochemistry *34*, 593–599.
27. Fletcher, T.M., Cathers, B.E., Ravikumar, K.S., Mamiya, B.M., and Kerwin, S.M. (2001). Inhibition of human telomerase by 7-deaza-2′-deoxyguanosine nucleoside triphosphate analogs: potent inhibition by 6-thio-7-deaza-2′- deoxyguanosine 5′-triphosphate. Bioorg. Chem. *29*, 36–55.

28. Seela, F., Soulimane, T., Mersmann, K., and Jurgens, T. (1990). 2,4-Disubstituted pyrrolo[2,3-*d*]pyrimidine α-D- and β-D-ribofuranosides related to 7-deazaguanosine. Helv. Chim. Acta *73*, 1879–1887.

29. Seela, F., Zulauf, M., and Chen, S.-F. (2000). Pyrrolo[2,3-*d*]pyrimidine nucleosides: synthesis and antitumor activity of 7-substituted 7-deaza-2′-deoxyadenosines. Nucleosides Nucleotides Nucleic Acids *18*, 1543–1548.

30. Balch, W.E., Der, C.J., and Hall, A. (1995). Small GTPases and Their Regulators. Part A. Ras Family, *Volume 255* (San Diego: Academic Press).

31. de Rooij, J., and Bos, J.L. (1997). Minimal Ras-binding domain of Raf1 can be used as an activation-specific probe for Ras. Oncogene *14*, 623–625.

32. Cuadrado, A., Bruder, J.J., Heidaran, M.A., App, H., Rapp, U.R., and Aaronson, S.A. (1993). H-Ras and raf-1 cooperate in transformation of NIH3T3 fibroblasts. Oncogene *8*, 2443–2448.

33. Tong, L.A., de Vos, A.M., Milburn, M.V., and Kim, S.H. (1991). Crystal structures at 2.2 Å resolution of the catalytic domains of normal ras protein and an oncogenic mutant complexed with GDP. J. Mol. Biol. *217*, 503–516.

34. Bos, J.L., de Rooij, J., and Reedquist, K.A. (2001). Rap1 signalling: adhering to new models. Nat. Rev. Mol. Cell Biol. *2*, 369–377.

35. Wohlgemuth, S., Kiel, C., Kramer, A., Serrano, L., Wittinghofer, F., and Herrmann, C. (2005). Recognizing and defining true Ras binding domains I: biochemical analysis. J. Mol. Biol. *348*, 741–758.

36. Letunic, I., Copley, R.R., Pils, B., Pinkert, S., Schultz, J., and Bork, P. (2006). SMART 5: domains in the context of genomes and networks. Nucleic Acids Res. *34*, D257–D260.

37. Finn, R.D., Mistry, J., Schuster-Bockler, B., Griffiths-Jones, S., Hollich, V., Lassmann, T., Moxon, S., Marshall, M., Khanna, A., Durbin, R., et al. (2006). Pfam: clans, web tools and services. Nucleic Acids Res. *34*, D247–D251.

38. Perez-Sala, D., and Rebollo, A. (1999). Novel aspects of Ras proteins biology: regulation and implications. Cell Death Differ. *6*, 722–728.

39. Reuther, G.W., and Der, C.J. (2000). The Ras branch of small GTPases: Ras family members don't fall far from the tree. Curr. Opin. Cell Biol. *12*, 157–165.

40. Fonagy, A., Swiderski, C., Wilson, A., Bolton, W., Kenyon, N., and Freeman, J.W. (1993). Cell cycle regulated expression of nucleolar antigen P120 in normal and transformed human fibroblasts. J. Cell. Physiol. *154*, 16–27.

41. Saijo, Y., Sato, G., Usui, K., Sato, M., Sagawa, M., Kondo, T., Minami, Y., and Nukiwa, T. (2001). Expression of nucleolar protein p120 predicts poor prognosis in patients with stage I lung adenocarcinoma. Ann. Oncol. *12*, 1121–1125.

42. Bantis, A., Giannopoulos, A., Gonidi, M., Liossi, A., Aggelonidou, E., Petrakakou, E., Athanassiades, P., and Athanassiadou, P. (2004). Expression of p120, Ki-67 and PCNA as proliferation biomarkers in imprint smears of prostate carcinoma and their prognostic value. Cytopathology *15*, 25–31.

43. Fonagy, A., Swiderski, C., and Freeman, J.W. (1995). Altered transcription control is responsible for the increased level of proliferation-associated P120 in rapidly growing breast carcinoma. Int. J. Cancer *60*, 407–412.

44. Ventura, L., Migaldi, M., Criscuolo, M., Castelli, M., Barolini, G., Ranieri, A., Bifaretti, G., Uboldi, P., and Leocata, P. (1999). Nucleolar protein p120 expression in oral carcinoma. Anticancer Res. *19*, 1423–1426.

45. Husson, H., Carideo, E.G., Neuberg, D., Schultze, E., Munoz, O., Marks, P.W., Donovan, J.W., Chillemi, A.C., O'Connell, P., and Freedman, A.S. (2002). Gene expression profiling of follicular lymphoma and normal germinal center B cells using cDNA arrays. Blood *99*, 282–289.

46. Sato, K., Nishi, T., Takeshima, H., Kochi, M., Kuratsu, J., Masuko, N., Sugimoto, Y., Yamada, Y., and Ushio, Y. (1999). Expression of p120 nucleolar proliferating antigen in human gliomas and growth suppression of glioma cells by p120 ribozyme vector. Int. J. Oncol. *14*, 417–424.

47. Trere, D., Migaldi, M., Montanaro, L., Pession, A., and Derenzini, M. (2000). p120 expression provides a reliable indication of the rapidity of cell duplication in cancer cells independently of tumour origin. J. Pathol. *192*, 216–220.

48. Perlaky, K., Valdez, B.C., Busch, R.K., Larson, R.G., Jhiang, S.M., Zhang, W.W., Brattain, M., and Busch, H. (1992). Increased growth of NIH/3T3 cells by transfection with human p120 complementary DNA and inhibition by a p120 antisense construct. Cancer Res. *52*, 428–436.

